https://doi.org/10.2352/ISSN.2470-1173.2018.11.IMSE-459


# Characterization of Image Sensor Resolution by Single-Pixel Illumination

*Victor Lenchenkov[1], Orit Skorka[1], Robert Gravelle[2], Ulrich Boettiger[3], and Radu Ispasoiu[1];*
*ON Semiconductor, Image Sensor Group, [1]San Jose, CA, USA; [2]Meridian, ID, USA; [3]Nampa, ID, USA*

## Abstract

*This work presents a method to characterize the 2D modulation transfer function (MTF) of electronic imaging systems using a setup that enables single-pixel illumination. The method is based on direct capture of point-spread function (PSF) images; therefore, it allows a higher level of accuracy than methods that derive PSF from multiple line-spread function measurements with a slanted-edge or another macro-target. The work presents a design of a measurement setup for PSF characterization, and a simulation test bench that can be used to simulate PSF. It shows simulated PSF images of 1.1 µm pixel pitch monochrome image sensors with and without µ-lenses, and the 2D-MTF plots that were calculated from these results. It also presents PSF images that were obtained from experimental work with these sensors and the 2D-MTF plots that were calculated for them. 1D-MTF results of the two sensors, as obtained from the slanted edge method, are compared to their cross-section 2D-MTF results, as obtained from PSF measurements. Comparison shows that there is a good agreement between the two methods, specifically, for measurements that are done with green light, and that the 2D-MTF method is more sensitive to spectral variations of the illumination.*

## Introduction

Spatial resolution is an important metric of imaging systems in a wide range of applications. These days, the slanted-edge method is commonly used as an industrial standard to quantitatively evaluate the ability of an imaging system to resolve fine details in a target [1]. This method extracts the line-spread function (LSF) of an imaging system by analyzing the system response to a slanted edge image that is projected on the image plane. The algorithm for image analysis includes summation and averaging, which results in loss of information. In addition, this method is prone to error due to variations in the tilt angle of the slanted edge [2].

As the slanted edge method requires high contrast levels, it cannot be used to characterize spatial resolution at varied contrast levels. However, characterization of this metric for the entire dynamic range of an imaging system, from low-light to very bright scenes, is especially important for automotive and surveillance applications.

The laser speckle is another method that has been developed to characterize MTF [3]. But this method is not easy to implement because it is quite technically and computationally challenging.

This work presents a setup for single-pixel illumination that enables direct capture of point-spread function (PSF) images for 2D-MTF analysis; its design is based on principles from physical optics, where light is treated as a combination of plane waves [4]. The setup is rather simple to implement and automate. This characterization method has no restrictions on contrast. It is sensitive to pixel structure and wavelength of the illuminating light. The method can be extended to include measurement of the pixel quantum-efficiency, blooming, lag, and dynamic range and, in general, can be used as a tool for design optimization.

## Principles of Image Formation

The 2D spatial frequency response of image sensors and imaging systems may be characterized through their PSF. The PSF represents the system response to a point source and that is, essentially, the impulse response of the system.

Formation of a point source on the image plane is not realistically possible. However, in digital image sensors, formation of a Gaussian irradiance pattern with a full-width at half-maximum (FWHM) that is smaller than the pixel area between the boundaries of a single pixel would produce a response that approximately represents the impulse response of the pixel array. To obtain an irradiance pattern with Gaussian shape on the image plane, one must form a Gaussian irradiance pattern at the entrance pupil in the rear side of the lens. The lens acts as Fourier transformer [5], and forms an image of the spatial spectrum of the object at the back focal plane. The Fourier transform of a Gaussian is a Gaussian.

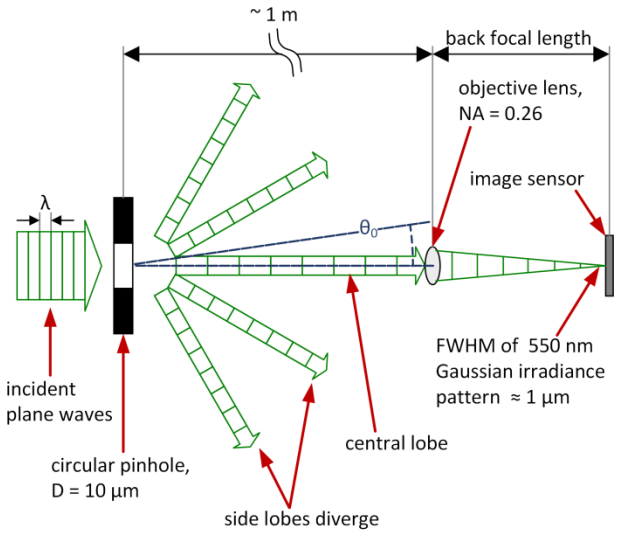


*Figure 1 – Airy disk pattern is obtained at the exit of the circular pinhole. The setup is designed so that only the central lobe, which can be approximated as a Gaussian irradiance pattern, passes through the microscope objective lens that acts as a Fourier transformer block. The Gaussian irradiance pattern, which is formed at the back focal length, can be used to characterize the impulse response of the image sensor if its FWHM is smaller than pixel size and the setup is perfectly aligned to enable single-pixel illumination.*

A circular aperture, which also acts as a Fourier transformer [5], can be utilized to form an irradiance pattern with Gaussian shape at the entrance pupil, if it is placed at a sufficient distance from that surface. Figure 1 illustrates a setup for single-pixel

illumination, where the example is given for light in the visible band, and pixel size in the image sensor under test is 1.1 μm.

When the plane waves pass through the circular aperture, the irradiance pattern at the other side of the aperture is, approximately, an Airy disk [6]. The total angular width of the first dark ring, $2\theta_0$, which represents the boundary of the central lobe, is given by:

$$2\theta_0 = 2.44\frac{\lambda}{D}, \quad (1)$$

where λ is the wavelength and $D$ is the aperture diameter. Using λ = 550 nm and D = 10 μm, one obtains $2\theta_0 = 0.1342$ rad. Therefore, $\theta_0 = 3.84^0$. At a distance of 1 m from the aperture, the radius of the central lobe is $r_0 = \tan\theta_0 = 67.1$ mm. To prevent the surrounding lobes from entering the lens, the diameter of the entrance pupil of the lens must be smaller than $2r_0$, which is 134.2 mm. In the measurement setup, entrance pupil diameter was smaller than 32.2 mm, which fulfills the requirement.

The central lobe of an Airy disk can be approximated by a Gaussian irradiance pattern [7]. The diameter of the Airy disk that is formed at the back focal length of the lens, $d_{bf}$, is given by:

$$d_{bf} = 2.44\frac{\lambda}{2\mathrm{NA}}, \quad (2)$$

where NA is the numerical aperture of the lens. With NA = 0.26, $d_b$ = 2.58 μm. The FWHM of the Gaussian irradiance pattern that is formed on the image plane at the back focal length may be calculated as follows:

$$\mathrm{FWHM}_{bf} = 1.03\frac{\lambda}{2\mathrm{NA}}. \quad (3)$$

This gives that $\mathrm{FWHM}_{bf}$ = 1.01 μm, which is smaller than the pixel pitch. The FWHM of the irradiance pattern that enters the image plane is even smaller because of the higher refractive index of the materials that it travels through. For example, at 550 nm, the refractive index of materials that are commonly used to fabricate μ-lenses is about 1.6, and the refractive indices of SiN and $SiO_2$, which are typically deposited on the surface that faces the light, are 2 and 1.5, respectively.

The optical transfer function (OTF), which is the 2D spatial frequency response of an imaging system, is the normalized Fourier transform of the system PSF, and the 2D-MTF of the system is the modulus of the OTF [5]. To calculate the OTF from the PSF, the Matlab embedded function *psf2otf* was used in this work with subsequent processing steps. This function is based on calculation of the discrete fast Fourier transform [8]. Subsequent processing included amplitude normalization and folding of the 2D spatial frequency range from central 0 to Nyquist frequency at the outer boundary.

## PSF Simulation

PSF simulations were done using the FDTD Solutions tool in *Lumerical* [9]. The test bench included a 15×15 array of 1.1 μm back side illuminated (BSI) CMOS image sensor with monochrome pixels and a point light source (dipole). Two grid structures were simulated: structure (a) has a planar image plane whereas, in structure (b), there is a μ-lens above each pixel on the side that faces the light, which is the back side of the image sensor. Both structures are shown in Figure 2.

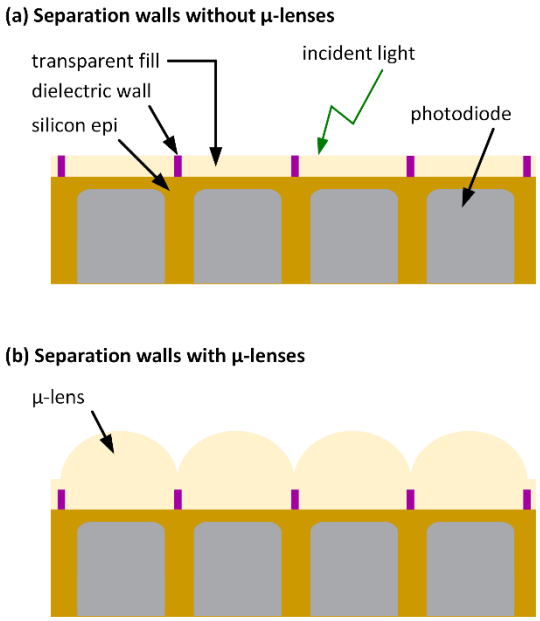


*Figure 2 – The two grid structures that were used in this work. The only difference between the two is that grid structure (a) has a planar surface, whereas grid structure (b) includes μ-lenses.*

To simulate the PSF of the pixel array, entrance of light was blocked from all but one pixel by covering the entire image plane with an opaque material (metal) while leaving a single opening, which is smaller than a pixel area, above the center of one of the pixels. Figure 3 presents the simulation test bench with grid structure (b).

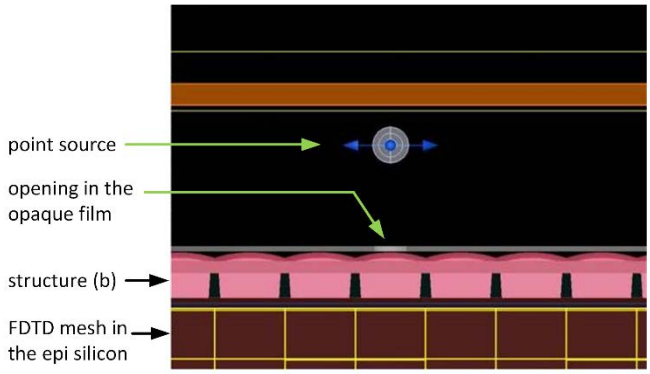


*Figure 3 – PSF simulation test-bench in the Lumerical FDTD Solutions tool. A point light source was placed above the center of the single pixel to which entrance of light was enabled through an opening in the opaque metal film*

Figure 4 presents simulated PSF results for grid structures (a) and (b) with 550 nm illumination. Signal level of the single pixel that is illuminated is similar in both structures. One may conclude from the plots that signal level of the closest neighbors is lower in grid structure (b), and this indicates that it surpasses grid structure (a), which does not have μ-lenses, at the ability to resolve fine details.

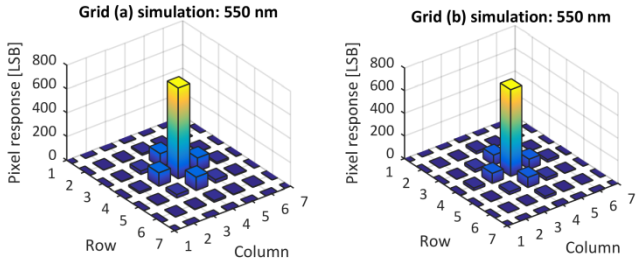


*Figure 4 – PSF simulation results of grid structures (a) and (b) with a 550 nm illumination source. Signal levels of the closest neighbor of the illuminated pixel in grid structure (b), which includes µ-lenses, is lower than in (a). Therefore, its spatial resolution is expected to be higher.*

Figure 5 presents the 2D-MTF plots that were calculated for the simulated PSF of grid structures (a) and (b) in Matlab. With grid structure (b), values at high spatial frequencies are higher, which is in agreement with expectations from PSF results. Figure 6 presents a cross section of the 2D-MTF plots to simplify comparison of the results. Also here, the advantage of having µ-lenses is obvious at high spatial frequencies.

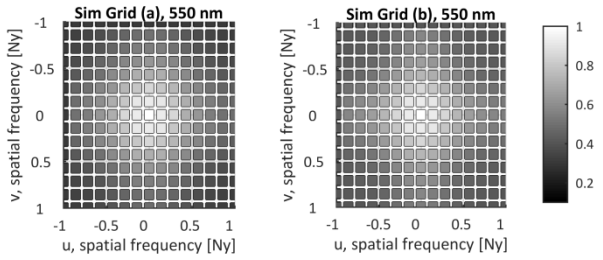


*Figure 5 – 2D-MTF of the simulated PSF curves of grid (a) and (b), respectively. At high spatial frequencies, grid (b), which includes µ-lenses, has higher 2D-MTF; therefore, its spatial resolution is superior to that of grid (a)*

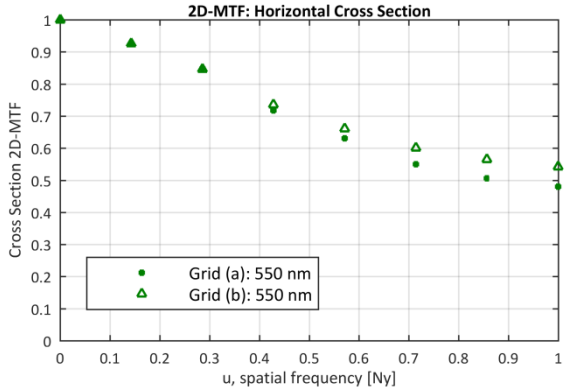


*Figure 6 – Horizontal cross-section of the 2D-MTF plots that were calculated at v = 0 for the simulated PSF images. The µ-lenses make grid (b) advantageous at high spatial frequencies.*

## Experimental Work

PSF of two image sensors with grid structures (a) and (b) was characterized using a setup that included a halogen light source, a collimator, a pinhole with aperture diameter of 10 µm (PNH-10), and three narrowband color filters with 40 nm FWHM centered on 450, 550, and 650 nm. The light beam was focused on the image plane using a Mitutoyo M Plan APO NIR 10x long-working distance microscope objective lens. Figure 7 shows photos of the test setup. The distance between the pinhole to the entrance of the objective was approximately 41" (1.04 m).

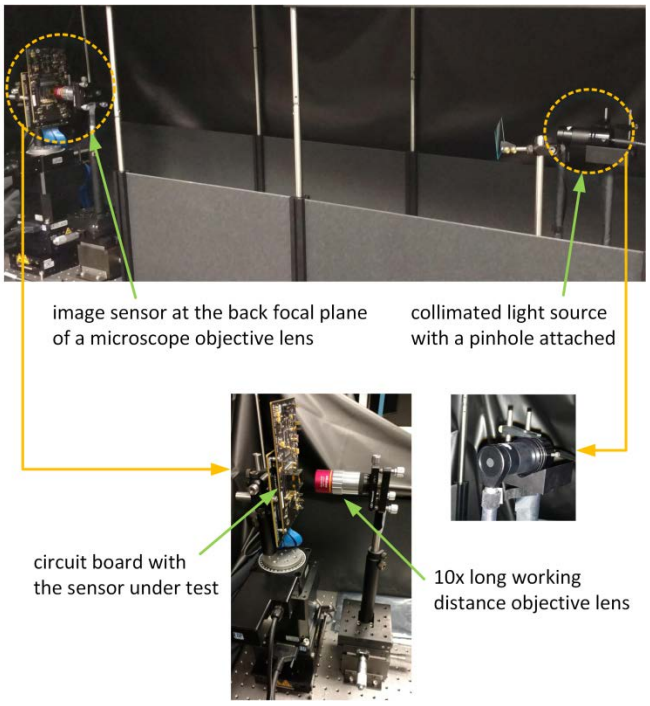


*Figure 7 – The setup that was developed for PSF characterization.*

The image sensors were accommodated in LBGA packages. At the beginning of each test procedure, the sensor was first aligned by changing its rotation angles until the response of all neighboring pixels to the one that was selected for PSF characterization had very similar signal level. Afterwards, to find focus location, sensor position was changed along the optical axis until it was possible to identify the location at which signal level of the selected pixel was maximal. A 30-frame average image was saved, where averaging was applied to filter out temporal noise. A 30-frame dark image was also saved and later used for pixel-wise dark level subtraction to minimize the effect of offset variations. Using a motorized positioning system, sensor position was varied perpendicular the optical axis in order to locate the position at which the center of the light spot was, in close approximation, the center of the pixel. This procedure was repeated with each image sensor and after each time a color filter was replaced.

At first, the setup accuracy was verified as follows: after fine alignment, sensor position was varied perpendicular to the light source using a motorized positioning system with a 50 nm step size. A 30-frame average image was captured at each position. Figure 8, Figure 9, and Figure 10 show the results after pixel-wise dark level subtraction, in LSB units, under blue, green, and red light, respectively, for grid (a) in the top row and grid (b) in the

bottom row. The two image sensors have 10-bit ADC resolution and pedestal level of 42 LSB. Other than dark level subtraction, no further processing was applied; therefore, these images represent raw pixel data.

Three positions were selected from each image set: position #1, which represents system position after fine alignment, the position at which signal level of the central pixel and its neighbor on the consecutive column on the same row was closest, and the position at which signal level of the neighbor pixel was maximal. In the top row of Figure 8, grid (a) results show that at position #11, i.e., at a lateral shift of 500 nm from the origin, which is about half pixel size, the power is distributed almost equally between the central pixel and its neighbor and, at position #22, i.e., at a lateral shift of 1050 nm from the origin, which is about one pixel size, signal level of the neighbor pixel is maximal and equal to signal level of the central pixel in position #1. One may conclude from this and similar results that are shown in Figure 8, Figure 9, and Figure 10 that the setup is repeatable.

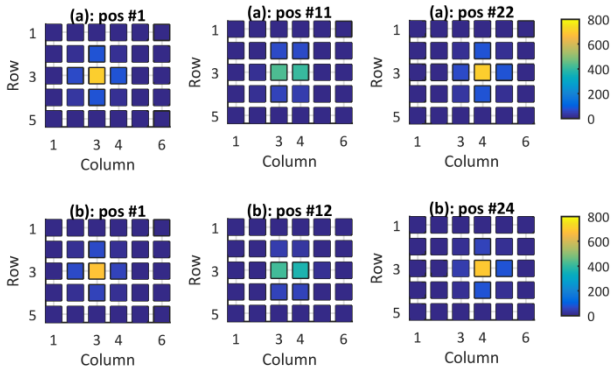


*Figure 8 – Sensor position was varied perpendicular to the light source with a motorized positioning system in step size of 50 nm. Grid (a) and (b) results are shown in the top and bottom rows, respectively, for the measurement that was done with a 450 nm filter. After a shift distance that equals one pixel size, signal level of the neighbor pixel is maximal.*

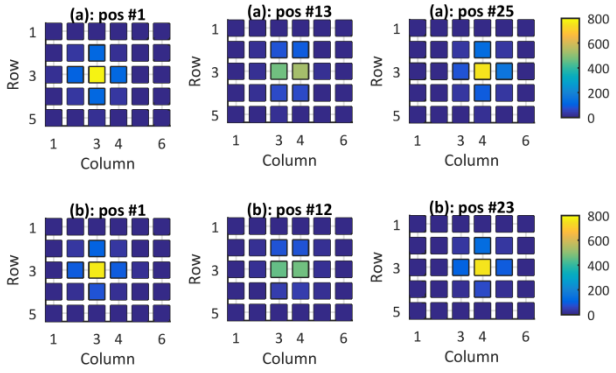


*Figure 9 – Sensor position was varied perpendicular to the light source with a motorized positioning system in step size of 50 nm. Grid (a) and (b) results are shown in the top and bottom rows, respectively, for the measurement that was done with a 550 nm filter. After a shift distance that equals one pixel size, signal level of the neighbor pixel is maximal.*

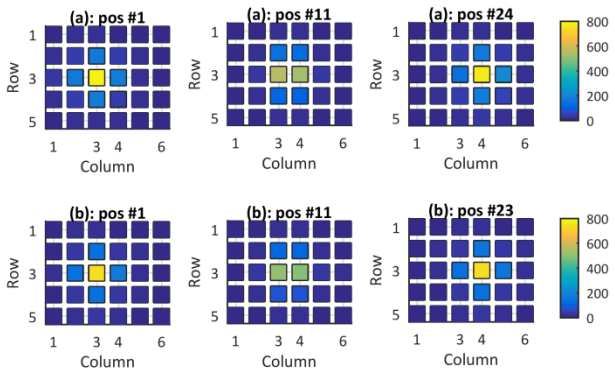


*Figure 10 – Sensor position was varied perpendicular to the light source with a motorized positioning system in step size of 50 nm. Grid (a) and (b) results are shown in the top and bottom rows, respectively, for the measurement that was done with a 650 nm filter. After a shift distance that equals one pixel size, signal level of the neighbor pixel is maximal.*

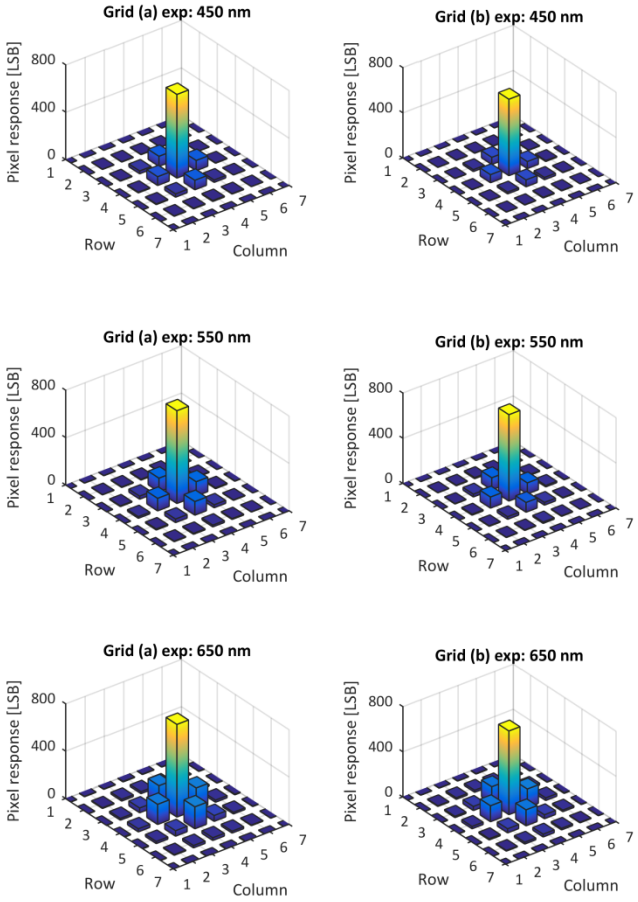


*Figure 11 – Captured single-pixel illumination images with the two grid structures using a narrow-band color filter with a central wavelength of 450, 550, and 650 nm. Results show that grid structure (b), which includes μ-lenses, has higher PSF for normal incident light in the center of the array. They also show that there is degradation in PSF with increase in wavelength of the incident photons.*

Figure 11 presents images of pixel response, in LSBs, after pixel-wise dark level subtraction. PSF measurements at 550 nm are in agreement with simulation results. Experimental results show that there is degradation in PSF with increase in wavelength. This is expected as longer wavelengths are absorbed deeper in the silicon substrate; therefore, they have a longer travel distance and more chances to be absorbed in a neighboring pixel.

Figure 12 presents 2D-MTF plots that were calculated for the captured PSF images. With both image sensors, the degradation in spatial frequency response with increase in wavelength is clear, specifically, for red illumination. Figure 13 shows horizontal and vertical cross-sections of the 2D-MTF plots. Results with the 550 nm filter are in very good agreement with simulation predictions. One may conclude that horizontal and vertical response curves are not identical. This stems from pixel and array layout design, which has differences along the column and row axes. The directional differences are more pronounced in structure (b), which includes μ-lenses.

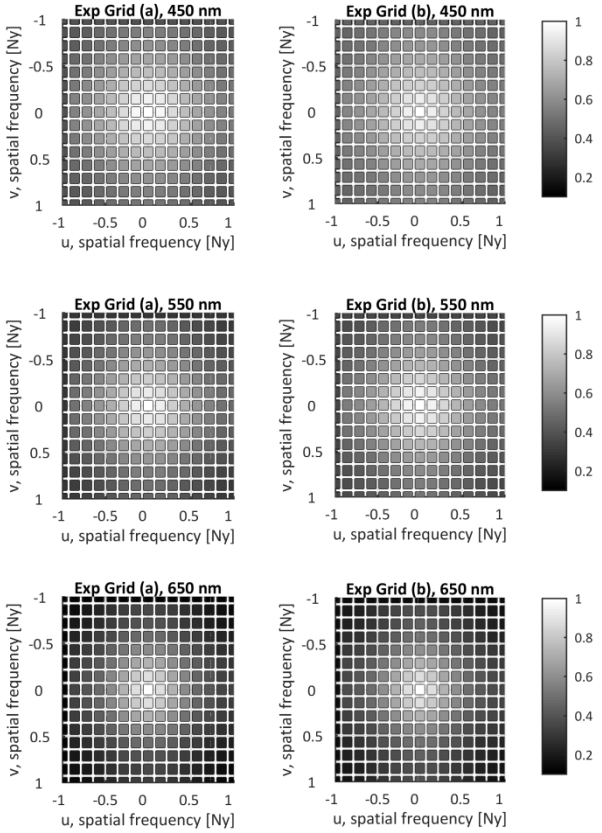


*Figure 12 – 2D-MTF of the PSF images that were captured in an experiment that was done with the two image sensors. 2D-MTF of the one that includes μ-lenses, grid (b), is higher at high spatial frequencies. Results show degradation in spatial resolution with the increase in the central wavelength of the illumination. They also show that there are differences between the spatial frequency response along the vertical and horizontal directions.*

1D-MTF of image sensors with grid structures (a) and (b) was characterized using the slanted edge method. Measurements were done with a halogen light source, the same narrow-band 450, 550, and 650 nm filters with 40 nm FWHM, and the same objective lens that was used in the setup for PSF characterization. The slanted edge image was projected at the center of the array and the region of interest for data analysis included 120×80 pixels. Sensor position was varied through focus, and the curve with the highest MTF was chosen to represent sensor performance. Measurements were done horizontally and vertically, and the *Imatest* software v4.4.5 was used in monochrome mode to analyze the results [10]. Lens MTF was assumed to be diffracted limited, therefore, it was divided from the original results to obtain image sensor MTF.

Figure 14 presents 1D-MTF results, as obtained from LSF analysis, and compares them to cross-section 2D-MTF results. For simplicity, the 1D and 2D-MTF curves in this figure represent the average of the horizontal and vertical curves in each case. Relative comparison shows that both methods agree that, at high spatial frequencies, grid (b) is superior to grid (a), and that there is degradation in MTF with increase in the central wavelength of the illumination. Absolute comparison shows that the PSF-based method is much more sensitive to spectral variations than the LSF-based method as 2D-MTF. Under green illumination, differences between 1D and 2D-MTF curves are rather small. This is beneficial because this is the wavelength band that is most important to human vision, and because the slanted edge method is well established [1] and easy to implement. However, at high spatial frequencies, blue illumination results show that the 2D-MTF values are higher than 1D-MTF, and red illumination results show that 2D-MTF values are lower than 1D-MTF.

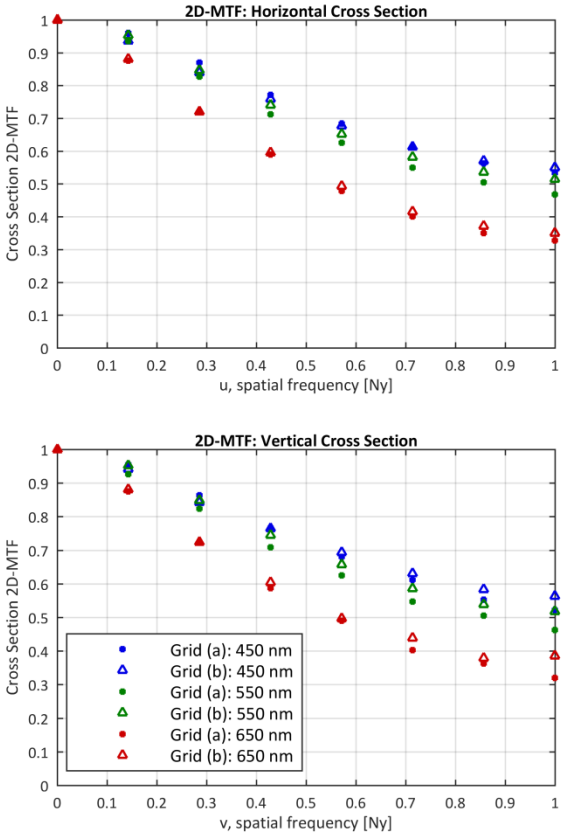


*Figure 13 – Horizontal and vertical cross-sections of the 2D-MTF plots, at v = 0 and u = 0, respectively, that were calculated for the experimental PSF captures. Grid (b), which includes μ-lenses, shows superiority to grid (a) at high spatial frequencies, and this is more pronounced in the vertical cross-section.*

The reduced sensitivity of the LSF-based method may be the outcome of the image capture procedure and analysis algorithm. During image capture, the pixels that are used for LSF analysis are partially illuminated in a non-uniform way. However, the different portions of the pixel layout affect MTF differently. The effect of each element is lessened because the overall response is averaged for data analysis. The PSF-based method is advantageous over the LSF-based one because it allows characterization of the spatial frequency of a single pixel with all the films, structures, and regions that compose a single pixel. This enhances measurement accuracy.

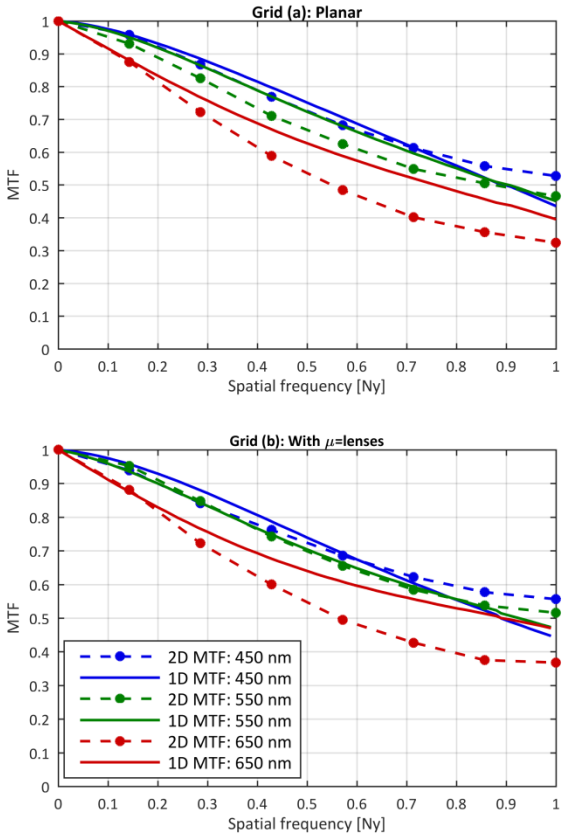


*Figure 14 – 1D-MTF curves that were calculated from slanted-edge images with three narrow-band color filters are compared to the cross-section of the 2D-MTF curves. Relative comparison shows that both methods agree that grid (b) shows superiority to grid (a) at high spatial frequencies, and that there is degradation in MTF with increase in wavelength. Absolute comparison shows that the PSF method is more sensitive to wavelength variations than the LSF one.*

## Conclusion

This work discusses characterization of the 2D-MTF of an imaging system from PSF images. It introduces a measurement setup that can be used to capture PSF images, and explains the design using principles from physical optics. A simulation test-bench was developed in Lumerical and simulated PSF results are shown for a 550 nm point source and 1.1 μm monochrome pixels with two grid structures: planar and with μ-lenses. The work presents an actual measurement setup and PSF images that were captured with these image sensors using light with central wavelength of 450, 550, and 650 nm. 2D-MTF was calculated for all PSF images, simulated and experimental ones. Simulated and experimental results are in good agreement; both conclude that μ-lenses allow enhancement of spatial resolution and that spatial resolution degrades with the increase in wavelength. Lastly, the work presents 1D-MTF results as obtained with the slanted edge characterization method. 1D-MTF results also agree that spatial resolution benefits from having μ-lenses and that MTF degrades with increase in central wavelength. However, absolute comparison between 1D-MTF and cross-section of 2D-MTF shows that the PSF method is more sensitive to wavelength variations than the LSF one. While the LSF method is based on non-uniform pixel illumination and averaging, the PSF method allows accurate characterization of a single pixel.

## References


[1] *ISO 12233:2017 Photography -- Electronic still picture imaging -- Resolution and spatial frequency responses,* 2017.

[2] Y. Duan, X. Xue, Y. Chen, L. Tian, J. Zhao and L. Gao, "Non-uniform sampling knife-edge method for camera modulation," *Proc. of SPIE,* vol. 10023, pp. 100231C 1-9, 2016.

[3] X. Chen, N. George, G. Agranov, C. Liu and B. Gravelle, "Sensor modulation transfer function measurement using band-limited laser speckle," *Optics Express,* vol. 16, pp. 20047-20059, 2008.

[4] S. A. Akhmanov and S. Y. Nikitin, Physical Optics, Clarendon Press, 1997.

[5] J. W. Goodman, Introduction to Fourier Optics, Roberts & Company Publishers, 2005.

[6] M. K. Kim, "Chapter 2: Diffraction and Fourier Optics," in *Digital Holographic Microscopy*, Springer, 2011, pp. 11-28.

[7] B. Zhang, J. Zerubia and J.-C. Olivo-Marin, "Gaussian approximations of fluorescence microscope point-spread function models," *Applied Optics,* vol. 46, pp. 1819-1829, 2007.

[8] MathWorks, "2017b Documentation," 2017. [Online]. Available: https://www.mathworks.com/help/images/ref/psf2otf.html?s_tid=srch title.

[9] Lumerical. [Online]. Available: https://www.lumerical.com/.

[10] Imatest. [Online]. Available: http://www.imatest.com/.


## Author Biography

*Victor Lenchenkov received the M.Sc. degree in chemical-engineering from Mendeleyev University of Chemical Technology, Russia, and Ph.D. in chemistry from the University of Southern California, USA. In 2002-2005, he was a postdoctoral researcher in the ultrafast spectroscopy group at Emory University. Since 2005, he is has been working on simulations and characterization of CMOS image sensors. He authored 18 patents and several publications in fields of imaging, physical optics, and ultrafast electronic and vibrational spectroscopy.*

*Orit Skorka received her BSc from Ben-Gurion University of the Negev, Israel, in 2001, her MSc from the Technion IIT, Israel, in 2004, and her Ph.D. from the University of Alberta, Canada, in 2011, all in Electrical and Computer Engineering. She joined Aptina in 2013 and is now with the Image Sensor Group at ON Semiconductor working on pixel characterization and image quality of CMOS image sensors for mobile imaging and automotive applications.*

*Robert Gravelle received his B.S.E.E. from University of Colorado at Colorado Springs. Bob joined Micron Technology in 1991 where he worked as a Parametric Engineer with DRAM and FLASH wafer processing until 2003 when he joined Micron's imaging group. Prior to ON's acquisition of Aptina Imaging, he managed the Optical Design and Characterization team. His current position is Member of Technical Staff, Optical Pixel Engineering. He has developed several modeling techniques for evaluating optical pixel response, characteristics and interaction of pixel and lens design.*

*Ulrich Boettiger is currently a Principal Member of Technical Staff at ON Semiconductor in Nampa, Idaho. He received his M.Sc. degree in Physics from University of Stuttgart / Germany in 1981. He joined IBM Germany's research lab in Boeblingen in 1981, working on bipolar and CMOS semiconductor R&D. In 1998 he joined Micron Technology in the US to initially work on advanced lithography and materials R&D. In 2001 he moved to the newly formed image sensor group and spear headed Micron's, later Aptina Imaging's and now the ON Image Sensor Group's pixel optics technology development. He was appointed a Micron Fellow in 2001 and an Aptina Fellow in 2013 and holds well over 100 patents.*

*Radu Ispasoiu is a senior manager of pixel R&D and image quality at ON Semiconductor ISG (since 2014). He has held engineering management and lead R&D positions in the Silicon Valley optoelectronics technology industry for more than 17 years. He holds a PhD in Physics (1996) with focus on semiconductor optoelectronic device study from the University of Oxford, UK.*